



## Relationship between the anisotropy of magnetic susceptibility and development of the Haymana Anticline, Central Anatolia (Turkey)

Murat ÖZKAPTAN<sup>1,2,\*</sup> , Erhan GÜLYÜZ<sup>3</sup> 

<sup>1</sup>Department of Geophysical Engineering, Faculty of Engineering, Karadeniz Technical University, Trabzon, Turkey

<sup>2</sup>Paleomagnetic Laboratory Fort Hoofddijk, Department of Earth Sciences, Utrecht University, Utrecht, the Netherlands

<sup>3</sup>Department of Geological Engineering, Faculty of Engineering, Van Yüzüncü Yıl University, Van, Turkey

Received: 06.03.2018 • Accepted/Published Online: 10.12.2018 • Final Version: 15.01.2019

**Abstract:** Integrated structural and anisotropy of magnetic susceptibility (AMS) analyses were carried out on the Campanian-Maastrichtian shale-mudstone dominated sedimentary sequences (Haymana Formation) cropping out within the doubly plunging Haymana Anticline in Central Anatolia (Turkey). In order to understand the relationship between the development of magnetofabrics and the tectonic processes, six sites from different parts of the anticline were sampled and analyzed. AMS lineations from 634 cylindrical samples and structural data were collected in the field. The results show very high correlation with the structural trend of the region and indicate that the maximum susceptibility vector ( $k_1$ ) is almost parallel to the Haymana Anticline fold axis (~E-W) and the trace of the Dereköy Thrust Fault, which is the basin-bounding fault at the northern margin of the Haymana Basin. In order to assess the relationship between shortening ratios and obtained AMS vectors, a number of balanced cross-sections are constructed along five traverses almost perpendicular to the axis of the anticline. Results from both the AMS and the balanced cross-sections yielded similar shortening ratios (~18%–32%) that decrease towards the eastern closure of the anticline from its culmination. In a regional sense, we related these results to compressional/transpressional deformation that formed during the Eocene to Early Miocene period. Differential shortening ratios calculated from AMS and restored balanced cross-sections indicate that the shortening is associated with the transcurrent tectonics, possibly in relation with rotational convergence of the Pontides and the Taurides and/or the oblique indentation of the Kırşehir Block into the Pontides during or subsequent to the collision.

**Key words:** Anisotropy of magnetic susceptibility, compressional tectonic, balanced cross-section, Haymana Basin, Central Turkey

### 1. Introduction

Anisotropy of magnetic susceptibility (AMS) for a rock sample is described by the directional variances of induced magnetization strength properties within a certain amount of ambient magnetic field (Hrouda, 1982). The orientation of the magnetic minerals is the main reason behind the magnetic directional variances within a rock unit. Technological advancement in the sensitivity of instruments has led to very sensitive, accurate, inexpensive, and fast measurements for the investigation of rock fabric designs. Therefore, the AMS technique as a paleomagnetic tool has been increasingly used for solving a wide range of geological problems, such as revealing the deformation histories of sedimentary basins (Borradaile and Tarling, 1981; Kissel et al., 1986; Hirt et al., 1995; Mattei et al., 1997).

The AMS technique can be applied to almost all types of rocks and provides nondestructive means for investigating petrofabrics and determining the mineral orientations in

a rock volume. Maximum anisotropy direction in well-deformed petrofabrics/grains is generally related to active tectonic forces and resultant macro/microstructures such as folds, faults, foliations, and lineations in rock volumes (Hrouda and Janak, 1976; Borradaile, 1988; Averbuch et al., 1992; Robion et al., 2007; Borradaile and Jackson, 2010). A potential area for AMS studies are accretionary prisms (similar to the geological settings of the Haymana Basin), which potentially have signs of various deformation events due to being involved in subduction processes in convergent systems hosting long-lived deformation events and/or resulting in them in adjacent regions (Hrouda, 1982; Housen and van der Pluijm, 1991; Pares et al., 1999; Pares and van der Pluijm, 2002, 2003; Housen and Kanamatsu, 2003; Hrouda et al., 2009; Özkaptan et al., 2018).

### 2.1. Geological setting and aims

Removal of two different branches of the Neo-Tethys Ocean in Central Anatolia gave way to intersection of three main

\* Correspondence: ozkaptan@ktu.edu.tr

tectonic blocks. These blocks are the Pontides (Eurasia) in the north, the Tauride Block (TB) of Gondwana in the south, and a triangular ( $a = 200$  km) tectonic domain in the center, namely the Kırşehir Block (KB) (also considered as a part of the Tauride Block), which is bounded by the Pontides and TB at the north and south, respectively (e.g., Ketin, 1966; Görür et al., 1984). These tectonic blocks are separated by two main suture zones called the İzmir-Ankara-Erzincan Suture Zone (IAESZ), between the TB, Pontides, and KB, and the Intra-Tauride Suture Zone (ITSZ), between the Kırşehir and Tauride blocks (Figure 1a), which is debatable (e.g., Aydemir and Ateş, 2006; Aydemir, 2009). Properly understanding the mechanism of the convergence between the African and Eurasian plates in Central Anatolia has been the main concern of some recent paleomagnetic studies (Bilim and Ateş, 2007; Meijers et al., 2010; Lefebvre et al., 2013; Bilim et al., 2015; Çinku et al., 2016; Hisarlı et al., 2016; Çinku, 2017). One of them, by Meijers et al. (2010), described the indentation of the Kırşehir Block into the Pontides along the IAESZ and the vertical block rotations on the Pontides caused by the indentation. Lefebvre et al. (2013) presented new evidence favoring the existence of the debatable ITSZ by paleomagnetic analysis of the Central Anatolian intrusions and found the original positions of them to be parallel to the proposed lineament of the ITSZ. Additionally and more importantly, they defined a new structural zone, the Hirfanlar-Hacıbektaş Fault Zone that dissects the KB into two sectors and gave way to today's geometric configuration of the Central Anatolian intrusions and Central Anatolia. This outcome is important for this study because Gülyüz (2015) also suggested that the structural zone described by Lefebvre et al. (2013) must extend into the Pontides by following the trace of the Dereköy Thrust Fault, which bounds the Haymana Basin in the north. A paleomagnetic study directly conducted on the basin infill of the Haymana Basin (Özkaptan, 2016) explained the vertical block rotations of the region and also gave a time constraint for them as Late Eocene to Early Miocene. These paleomagnetic studies mainly focused on the vertical block rotations in the region and shed some light on the convergence mechanism; however, no AMS study has been applied in Central Anatolia comparing local/regional strain changes with the regional tectonic scenarios.

The Haymana Basin is located between the Tauride Block and the Pontides and has an almost 7-km-thick Late Cretaceous to Eocene basin infill (Figure 1). It is considered as a forearc to foreland basin (e.g., Koçyiğit, 1991; Görür et al., 1998; Gülyüz, 2015), which initially evolved on an accretionary prism under the control of subduction during the Late Cretaceous to Paleocene and was later affected by continental collision events that occurred between TB-Pontides-KB and postcollisional further convergence

in the region until the Late Miocene (Kaymakçı et al., 2009; Gülyüz, 2015; Özkaptan, 2016). Although there is no direct contact between the Kırşehir Block and the Haymana Basin, the Dereköy Thrust Fault, one of the main basin-controlling faults, is considered as a structure that brought the indentation-related deformation (KB into the Pontides) into the basin. However, this scenario has not been supported by any quantitative results except from some slickenlines on the ~1-km-wide Dereköy Fault Zone indicating a left lateral sense (Gülyüz, 2015).

In the scope of the regional geological setting, this study focuses on the traces of these complex deformation events by obtaining both AMS and kinematic data in order to test the effects of the regional tectonic events on a local scale structure, the Haymana Anticline. The Haymana Anticline, in the core of which the Upper Cretaceous Haymana Formation is exposed, was selected because the formation, the oldest one in the basin, should have recorded total strain related to the cumulative tectonic load applied on the basin, and, being the most eroded fold in the region, the anticline is the most suitable locality that allows to take AMS samples from the core of the anticline (only cores of anticlines record the contraction-related deformation).

In addition to the testing of regional scale tectonic scenarios, this study also aims to understand the relationships between AMS and development of an anticline by comparing AMS results with restorations of balanced sections. Although the main outcome of an AMS study conducted on sedimentary sequences is generally considered to be an understanding of the deformation styles of the units by finding out the geometries of the strain ellipsoids of magnetic grains that are thought to be shaped under the control of post- or syndepositional deformation, another important but poorly documented outcome of such studies is the AMS-strain correlation, which is based on the finite strain calculations of magnetofabric structures by determining clustering levels in different anisotropy principle axes (Borradaile, 1991b; Passier et al., 2001; Evans et al., 2003; Hrouda et al., 2009; Tripathy, 2009). It basically allows to make interpretations about the shortening that occurred in the sedimentary sequences. Here, it was aimed to reach both outcomes of AMS. In addition, it is aimed to compare AMS-based shortening ratio calculations with those calculated from balanced cross-sections.

In this study, we present the first results of low magnetic field AMS analysis of the Haymana Formation in Central Anatolia, Turkey (Figure 1), and a case study comparing AMS-based and balanced cross-section-based shortening ratio calculations. Moreover, our magnetofabric deformation results and other independent structural data shed some light on the tectonic settings of the region in

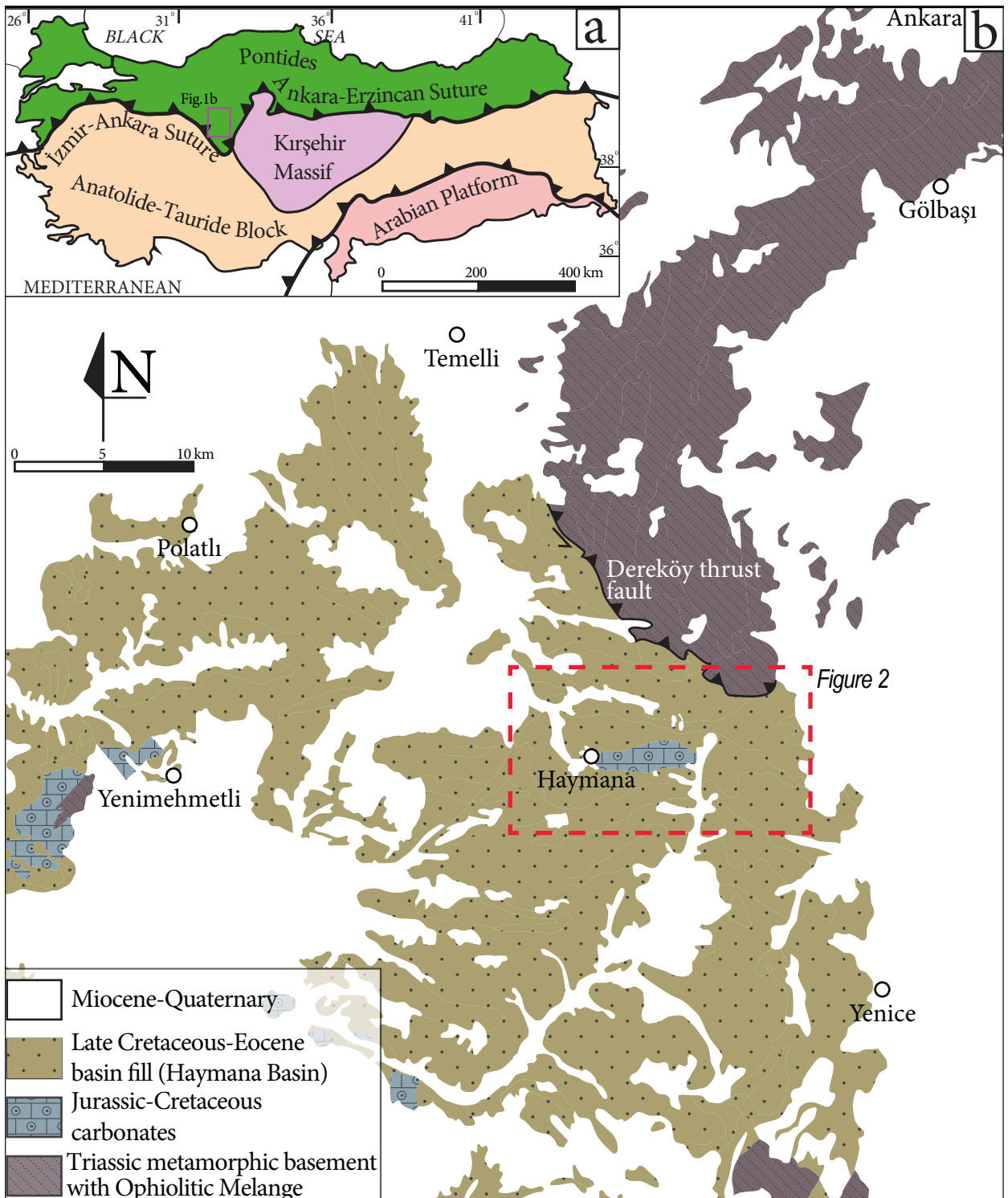


**Figure 1.** a) Major tectonic divisions of Anatolia modified from Görür et al. (1984); b) generalized geological map of the Haymana Basin, Central Anatolia (modified from 1/500,000 geological map of Turkey, MTA, 2002). The red dashed rectangle shows the boundary of detailed geological map of the study area in Figure 2.

association with the closure of the Neo-Tethys Ocean in Central Anatolia since the late Cretaceous.

2.1.1. Characteristics of the Haymana Formation

The Campanian-Maastrichtian Haymana Formation is the oldest turbiditic succession of the Haymana forearc to foreland basin and unconformably overlies Upper Jurassic–Lower Cretaceous pelagic limestones of the Pontides, which constitutes the core of the Haymana Anticline (Yüksel, 1970; Ünalın et al., 1976; Şengör and Yılmaz, 1981; Koçyiğit, 1991; Nairn et al., 2013; Rojay, 2013; Okay and Altiner, 2016) (Figure 1). While the total thickness of the basin is greater than 7 km by both field observation and geophysical data (Aydemir and Ateş, 2006; Aydemir, 2011), the Haymana Formation, which represents the base of the forearc deposition in the basin, is 1.8 km in thickness (Ünalın et al., 1976; Uygun, 1981; Koçyiğit, 1991; Görür et al., 1998). At the bottom, the formation is mainly composed of dark greenish to yellowish-brownish color, well-consolidated, fine-grained, thin-bedded shale-mudstone intercalations with frequent lens conglomerate, whereas at the upper levels of the succession, mudstone grades into shale-sandstone alternation and rare

conglomeratic successions are observed, both of which indicate a coarsening upwards trend for the formation (Figure 2).

The sampling locations in the Haymana Anticline, suitable for the aims of this study, were drilled only in one lithology that is composed of fine-grained mudstone-shale alternation. At two sites (SEC3 and SEC4), the samples were initially collected for magnetostratigraphic aging purposes. This allowed us to select the most suitable samples for AMS measurements since we knew the demagnetization characteristics of the specimens prior to AMS analyses. Knowing the approximate ages of the sampling locations for the two sampling sites together with the spatially distributed four sites made it possible to control strain changes by AMS in a spatiotemporal sense for the Haymana Anticline.

2.2. AMS-strain quantitative correlation

The strain characteristics related to the tectonic load of sedimentary rocks are commonly evaluated by clast-based measurements (X-ray, electron microbeam, etc.), which basically give information about the clast geometry and orientations, axial ratios, and the gaps between the clast

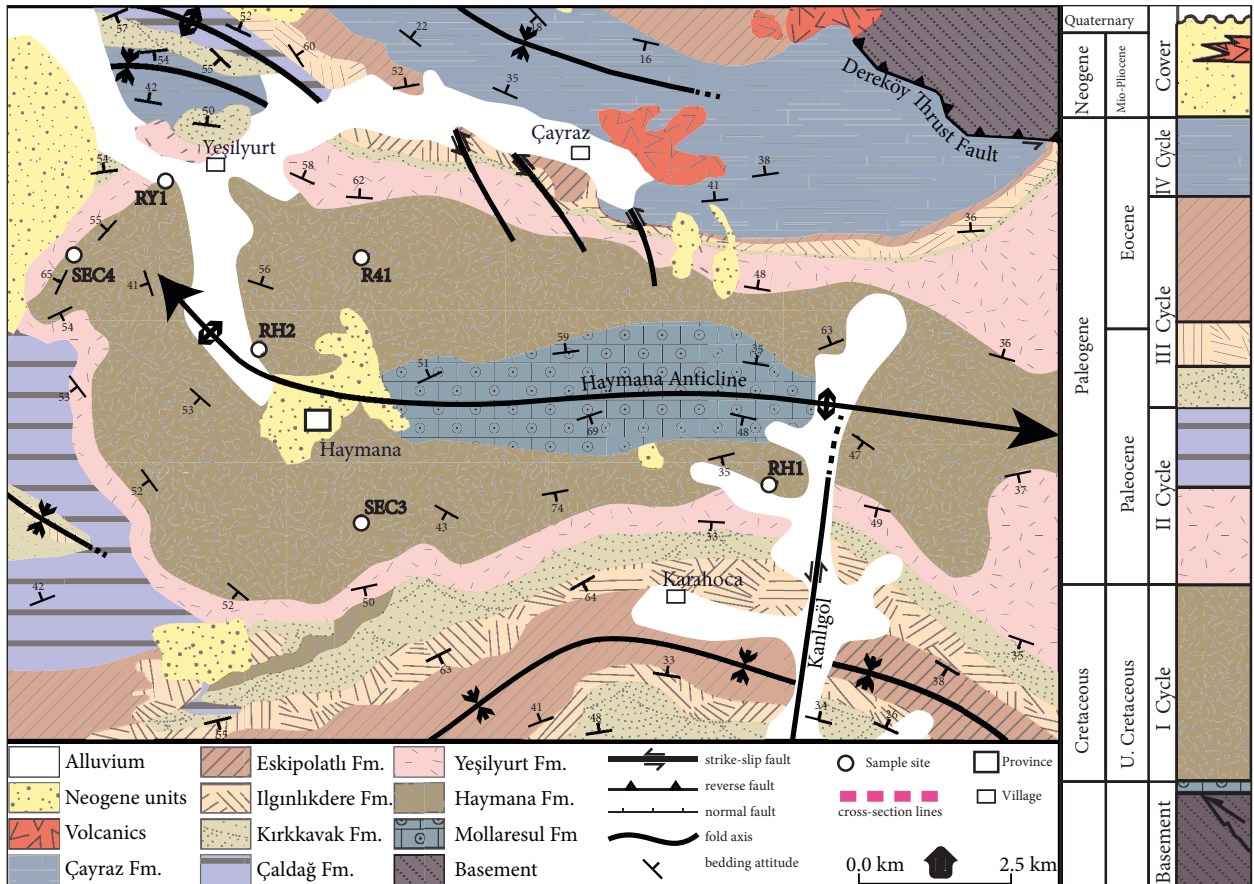


Figure 2. Detailed geological map of the study area modified from MTA (2002) and Ünalın et al. (1976).

center of deformed minerals and grains. A similar analogy is also followed for rocks including magnetic minerals. These minerals are stretched and reoriented and they can also be exposed to syndeformational recrystallization, which exhibits distinct magnetofabric patterns. All of these changes can be determined by AMS studies. The AMS method is generally applied to reveal qualitative relationships between magnetofabric design and strain accumulated in the rocks (e.g., Borradaile and Henry, 1997; Pares and van der Pluijm, 2002; Büyüksaraç et al., 2005). However, quantitative studies focusing on establishing empirical formulas to correlate between AMS and tectonic strain are very rare and poorly documented for all lithologies (e.g., Hrouda, 1982; Kissel et al., 1986; Borradaile, 1987, 1988, 1991; Housen and van der Pluijm, 1991; Tarling and Hrouda, 1993; Sagnotti et al., 1994; Housen et al., 1995; Aranguren et al., 1996; Pares et al., 1999; Pares and van der Pluijm, 2003, 2004). In general, there are two approaches followed for AMS-strain correlation: 1) a numerical approach using simulations for magnetofabric development (Owens, 1974; Richter, 1992; Benn, 1994), and b) an empirical approach, first proposed by Borradaile (1991). Both of these methods basically focus on the AMS shape parameter  $T$  as an indicator for finite strain calculated from magnetofabric structures under certain tectonic processes. The basic idea is to figure out the degree of clustering of the different anisotropy principal axes (particularly  $k_2$ ) for the low-to-moderately deformed sedimentary rocks (Housen et al., 1993; Pares et al., 1999). This type of study was applied on mudstones to determine the degree of shortening in the Appalachian Orogeny (Pares and van der Pluijm, 2003, 2004). The authors quantitatively proposed a strain-related exponential formula for the tectonic shortening: (%) =  $17 \times \exp(T)$  within confidence limits of 10%–25% up to 40%. If a sample is highly strained (strong cleavage), the  $T$  parameter becomes insignificant because similar results on principal axes orientations are found on such conditions. This problem might be overcome by using Woodcock diagrams representing clusters that have different distribution values in  $k_1$  axes (Woodcock, 1977; Pares et al., 1999; Oliva-Urcia et al., 2010); however, samples of this study, based on the shape of the AMS susceptibility ellipsoids/diagrams from six sites (Figure 3), show low to moderate levels of deformation. Therefore, the formula proposed by Pares and van der Pluijm (2003, 2004) is suitable for our sampled lithology.

### 3. Methods

#### 3.1. AMS sampling, measurement procedures, and methodology

In total, 634 standard core plugs from 6 different locations were sampled from the Haymana Formation. Depending

on the suitability of the sampling localities, a minimum of 22 and maximum of 266 oriented rock samples for each site were collected. Frequently single core lengths were enough to provide multiple specimens for AMS analyses.

The drilling orientations (plunge and azimuth) and bedding plane (strike and dip) were measured in the field with a magnetic compass corrected for secular variations (4.5°E, 2014). The sample isolation was guaranteed by sealing them with aluminum foil covers and transporting them in plastic bags.

The AMS measurements, as well as thermomagnetic measurements (Curie balance), were carried out at the Fort Hoofddijk Paleomagnetic Laboratory of Utrecht University in the Netherlands. Since AMS measurements are more dependent on the shape parameter than other paleomagnetic studies, our drilled samples were cut into the standard paleomagnetic measurement size (2.54 cm in diameter and 2.1 cm in height) and broken, jointed, and mixed-color ones were excluded from further analyses. Optimum height/diameter ratio for cylinders varies between 0.8 and 0.9 as suggested in previous studies (Noltimier, 1971; Scriba and Heller, 1978; Collinson, 1983). A total of 256 solid and crack-free specimens were measured in automatic field variations (low field, 200 A/m) using the Multifunction Kappabridge MFK1-FA (AGICO, Brno, Czech Republic). The sensitivity of the measurement is  $10^{-8}$  SI, which is critical for measurements in weak magnetic carriers like sedimentary rocks. During the measurements, the specimen is subsequently rotated between three perpendicular plane positions for the anisotropy and one for the bulk susceptibility as dictated by the spinning specimen measurement method. This gives an opportunity for computing the principal susceptibility axes of an AMS ellipsoid following the procedure introduced by Jelinek (1977). Between these steps, the bridge is calibrated to zero before inserting the specimen into the measuring coil. This allows determining both the differences between the steps more precisely and the susceptibility tensor, which can be enhanced by measurement at the lowest possible sensitive ranges. A complete susceptibility tensor is calculated by combining four values.

The AMS susceptibility or deformation ellipsoid is defined by three principal axes,  $k_1 \geq k_2 \geq k_3$  (or  $k_{\max} \geq k_{\text{int}} \geq k_{\min}$ ), namely the maximum, intermediate, and minimum susceptibility values, respectively. The shape of the magnetic susceptibility ellipsoid corresponds to these strain axes. When  $k_3$  is smaller than  $k_1$  and  $k_2$ , the shape of the AMS ellipsoid becomes oblate. In this case,  $k_3$  clusters perpendicular to the bedding plane, whereas  $k_2$  and  $k_1$  scatter parallel to the bedding plane. This pattern is commonly observed in undeformed fine-grained sedimentary rocks. Increase in the deformation range and other dynamic

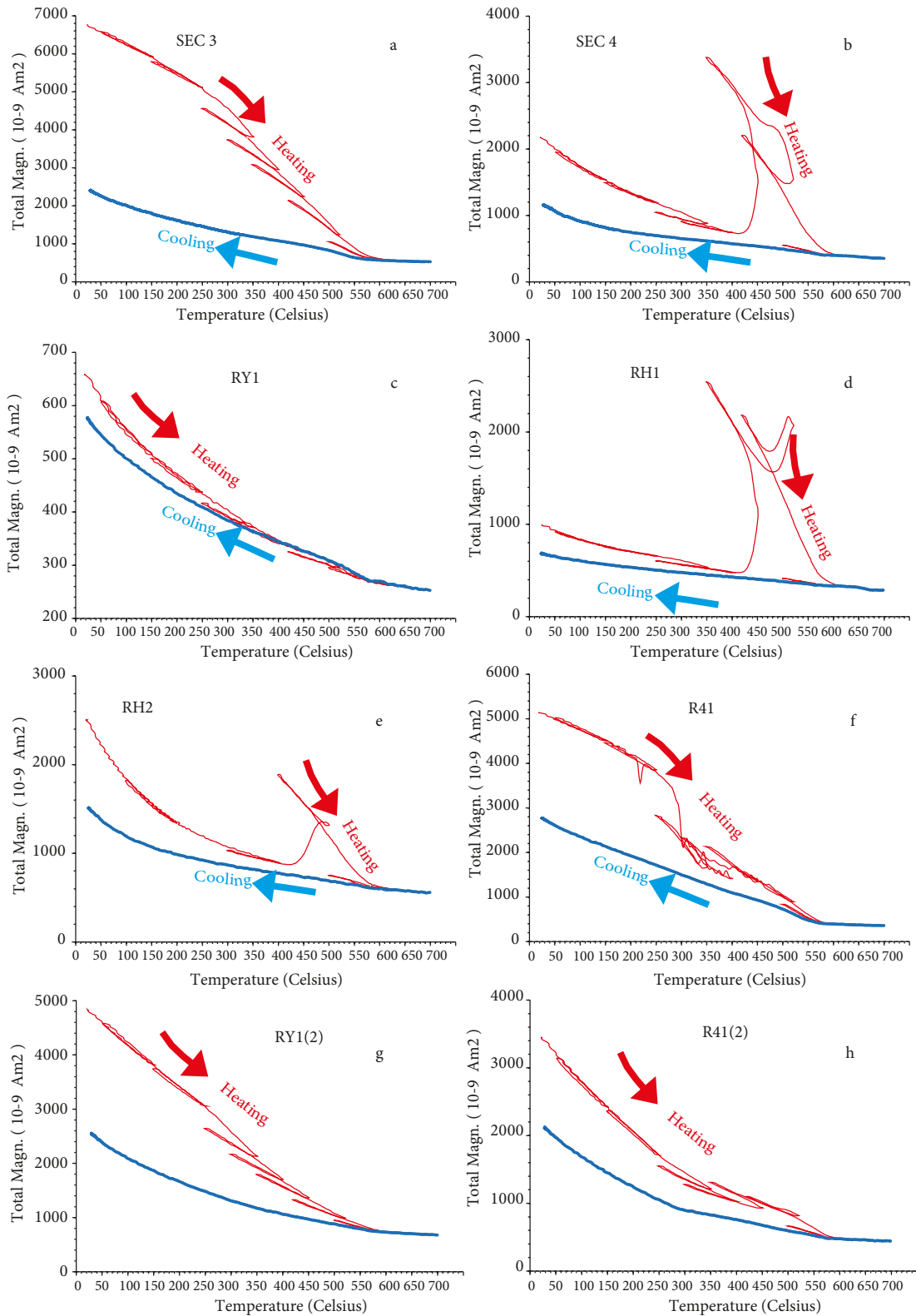


**Figure 3.** Total magnetization versus temperature curves generated with the segmented heating protocol (Mullender et al., 1993) for representative samples. The final cooling segment is indicated with blue line. See the text for explanation of the thermomagnetic behavior. The horizontal axis is the temperature scale and shows a change from room temperature to 650 °C. The vertical axis represents total magnetization depending on magnetic mineral content of specimens.

effects (i.e. paleocurrent or tectonic) transforms the oblate shape of the strain ellipsoid to a prolate shape. In such a case, the  $k_3$  axis is not perpendicular to the bedding plane; however, if it is observed as parallel or perpendicular to the bedding strike, the maximum extension directions (maximum compressional stress direction) are interpreted in weakly deformed sedimentary units, respectively.

All measured data, based on the specimens' coordinates and geographic and paleogeographic orientations, are first corrected. This concept is similar to tilting or bedding correction (also known as tectonic correction - TC) applied in routine paleomagnetic studies. The results from both specimen and the site means are analyzed by applying Jelinek statistics (Jelinek, 1977, 1978) and illustrated with the AniSoft 4.2 program (Chadima and Jelinek, 2009).

### 3.2. Thermomagnetic analyses

Thermomagnetic runs are executed to characterize dominant rock magnetic carriers (Curie temperatures) of the specimens. Total magnetization versus temperature runs (K/T curves) are utilized in air using a modified horizontal translation type Curie balance with a sensitivity of  $\sim 5 \times 10^{-9}$  Am<sup>2</sup> (Mullender et al., 1993). Procedures described by Huang et al. (2013) were followed in the study. Approximately 30–90 mg of powdered rock samples from six different levels of the Hayman Anticline were put into quartz glass sample holders and their tops were stoppered by quartz wool. The successive heating and cooling rates were 10 °C/min in air up to successively higher temperatures (max. 700 °C), and the specimens were finally cooled to room temperature. Stepwise thermomagnetic experiments were carried out with intermittent cooling between successive heating steps. Specimens were progressively heated (cooled) by successive temperature steps at 150 (50), 250 (150), 350 (250), 400 (300), 450 (350), 525 (420), 580 (500), and 700 °C (cooled until room temperature), respectively. Based on the thermomagnetic curves, Curie temperatures were determined following Fabian et al. (2013). Different from conventional thermomagnetic measurements (magnetic susceptibility), total magnetization measurements were analyzed and thus it was aimed to determine more detailed information about possible dominant magnetic mineral(s) by considering multiple phases rather than a single temperature curve.

### 3.3. Cross-section balancing of the Haymana Anticline

To reveal the three-dimensional geometry of the Haymana Anticline and precisely calculate shortening rates along with the different traverses, we constructed and restored five cross-sections. For this purpose, more than 500 bedding attitudes were measured from the study area, although only ~200 of them were used during cross-section constructions. Additionally, boundaries of stratigraphic cycles and a digital elevation model of the study area are

used as base data for constructing cross-sections. The trends of the sections are determined by considering the orientations of the fold (~E-W trending-double plunging) and the locations of the AMS samples calculated in order to compare shortening ratios of AMS results and those of cross-section studies. The reason for using the boundaries of the stratigraphic cycles rather than formation boundaries is the fact that the change of the locations of the transitions of lateral facies between the coevally deposited formations in the subsurface is unpredictable. The use of the stratigraphic cycle boundaries is therefore considered as a solution to overcome this problem because they are thought of as continuous lines tracing the same time interval in the subsurface. The characteristics and definitions of the stratigraphic cycles were given by Gülyüz (2015). These cycles were basically based on the depositional environment of the basin fill and their lateral/vertical stratigraphic continuity and were described as a group of shallow- and deep-marine deposits containing continental clastic rocks. Although more than 500 bedding attitudes were systematically collected from the anticline, during the construction only ~200 bedding measurements from 2-km-wide buffer zones of the section traces and the 30-m resolution digital elevation model taken from USGS open sources were used. The academic version of Midland Valley Move 2015.1 software was used both to construct and balance the sections. During cross-section constructions, only surface geological data were used and the geometry of 1B fold classes (parallel folding) of Ramsay (1967) was taken into account. This type of fold allows a constant bed height/thickness between the tops and bottoms of the strata. Postdepositional deformation occurring in the basins is generally recorded by 1B type folds (Dahlstrom, 1969) because the deformation in the upper level of the crust is not ductile and thicknesses of the sedimentary layers are preserved by layer-parallel flexural slip during folding procedures unless synsedimentary deformation does not affect the folding or the folded material does not flow. Thinning/thickening between strata are generally observed in metamorphic conditions. During restoration, a flexural-slip unfolding algorithm was used so that the area/thickness of the stratigraphic cycles and line length of the uppermost horizons (base of stratigraphic cycle 1) were preserved (c.f. Dahlstrom, 1969). This method assumes that internal deformation occurs mostly by layer-parallel slip and the amount of slip increases away from hinge lines of the folds, and it may briefly be explained by rotating the horizons to the horizontal direction by removing the flexural slip components of the fold. After the unfolding procedure, horizontal unfolded layers were used for shortening ratio calculations. The shortening ratio calculation is based on the formula  $(UL - DL) \times 100 / UL$ , where UL is the undeformed length of the section and DL is the deformed length of the section.

**4. Results**

**4.1. Thermomagnetic behaviors of the Haymana Formation**

Thermomagnetic experiments were carried out for each site and representative results of them are plotted in Figures 3a–3h. The thermomagnetic curves from different levels of the Haymana Formation show that samples have a heterogeneous mixture of magnetic carriers, which occur in varying amounts and proportions, in each level, and only one site (RY1) has rather low total magnetic intensity ( $\sim 680 \times 10^{-9} \text{ Am}^2$ ), probably due to the relatively small amount of magnetic minerals fraction in the specimen matrix (Figure 3c). From the total magnetization versus temperature diagrams, three types of curve are recognized: 1) magnetite is the dominant magnetic mineral since the major decrease occurs at  $\sim 575 \text{ }^\circ\text{C}$  (determined from the two-tangent method; Figures 3a, 3c, and 3g); 2) curves show sharp decreases in magnetization with Curie temperatures of  $\sim 350 \text{ }^\circ\text{C}$ , which indicates the presence of Ti-rich titanomagnetite as the magnetic carrier (Figures 3f and 3h); 3) in the last shape of the curves (Figures 3b, 3d, and 3e) is the typical example of a greigite dominant matrix showing a significant increase in intensity during the heating-cooling cycle at  $\sim 420\text{--}500 \text{ }^\circ\text{C}$  and totally removed after  $580 \text{ }^\circ\text{C}$  (decrease in magnetization with increasing temperature). Such an abrupt change is probably related to the conversion of paramagnetic iron sulfide and/or clay minerals into magnetite iron oxide as a new magnetic mineral phase. There are no distinguishable differences and all thermomagnetic curves are reversible in between heating and cooling phases after  $580$  up to  $700 \text{ }^\circ\text{C}$  due to dominance of paramagnetic mineral phases.

Briefly, the magnetic carriers of the specimens sampled in different stratigraphic levels are interpreted to be dominated by magnetite, titanomagnetite, and greigite. Since the samples were taken within at least a 250-m stratigraphic thickness, sedimentary environmental and/or source area changes are likely to vary in the dominant magnetic mineral properties stored in the rock. For example, presumably the dominance of greigite is related to more anoxic conditions and the hematite to paleosoils within the formation.

**4.2. Magnetofabric properties of the Haymana Formation**

The related AMS parameters (some explained above) and distributions of the deformation ellipsoids were computed for six sites following Jelinek statistics (Jelinek, 1978). The results and diagrams are reported in the Table. The site mean magnetic susceptibility ( $k_m$ ) of 6 sedimentary sites are highly homogeneous and range from  $78 \times 10^{-6} \text{ SI}$  to  $1300 \times 10^{-6} \text{ SI}$  (with more frequent values in the range of  $600\text{--}800 \times 10^{-6} \text{ SI}$ ), indicating a major contribution of the paramagnetism to a small percentage of ferromagnetic minerals of the rock composition to the bulk susceptibility (Borradaile et al., 1986; Rochette, 1987; Sagnotti et al., 1998) (Table; Figure 4a). The magnetic susceptibility magnitudes are relatively variable in each of the stratigraphic levels of the sedimentary strata. The degree of the AMS changes is independent of the stratigraphic positions but the magnitude is controlled by the nature of the rock matrix. The degree of anisotropy ( $P_j$ ) values are relatively low ( $\leq 1.1$ ) and change in a wide range from 1.1 to 1.025, indicating only initial to moderately developed magnetic fabric (Table; Figures 4a and 4b).

**Table.** Anisotropy of magnetic susceptibility results from the Haymana Anticline.

Site	Geog. coord.(deg)		$N_{AMS}$	Bedding Azi/dip	$k_m \times 10^{-6}$ (SI)	L	F	Pj	T	D/I ( $k_1$ )	D/I ( $k_3$ )	$e_1$	$e_2$	$e_3$	f (%)
	Lat. (N)	Long.(E)													
SEC3	39.42022	32.51139	80	131/37	0919.0	1.021	1.073	1.100	0.541	087.5/09.5	316.1/75.7	12.9	12.6	10.8	28.10
SEC4	39.46639	32.45941	27	228/49	0078.6	1.006	1.017	1.024	0.485	226.8/05.3	119.5/72.6	26.6	26.8	11.5	24.71
RY1	39.46935	32.46973	40	244/63	0140.0	1.012	1.015	1.027	0.107	251.9/10.1	116.5/76.0	12.5	12.6	08.1	18.44
RH1	39.41609	32.61153	31	125/48	0487.0	1.024	1.028	1.053	0.077	284.7/02.1	017.6/54.6	07.6	07.1	07.7	18.36
RH2	39.43985	32.48446	19	229/56	0614.0	1.013	1.068	1.088	0.666	266.1/04.3	140.0/82.8	13.6	13.2	07.2	32.24
R41	39.45675	32.51812	21	249/33	1300.0	1.004	1.027	1.033	0.767	279.6/20.2	091.3/69.6	44.7	44.8	16.5	28.61

Geographic coordinates are in WGS data; Lat. = latitude, Long. = longitude;  $N_{AMS}$  = number of specimens Bedding Azi = azimuth angle of the bedding, dip = dip angle of the bedding;  $k_m$  = mean susceptibility; L = magnetic lineation ( $k_1/k_2$ ); F = magnetic foliation ( $k_2/k_3$ ); Pj = corrected degree of anisotropy ( $\exp\sqrt{2[(n_1 - n)^2 + (n_2 - n)^2 + (n_3 - n)^2]}$ ) (Jelinek, 1981); T = shape parameter ( $2(n_2 - n_3)/(n_1 - n_3) - 1$ ) (Jelinek, 1981);  $e_1$  = semiangle of the 95% confidence ellipses around the principal susceptibility axes (Jelinek, 1981);  $n_1 = \ln k_1$ ,  $n_2 = \ln k_2$ ,  $n_3 = \ln k_3$ ,  $n = (n_1 + n_2 + n_3)/3$ ; D (declination) and I(inclination) for  $k_1$  and  $k_3$  after tectonic correction. f indicates shortening value (%) of each site.



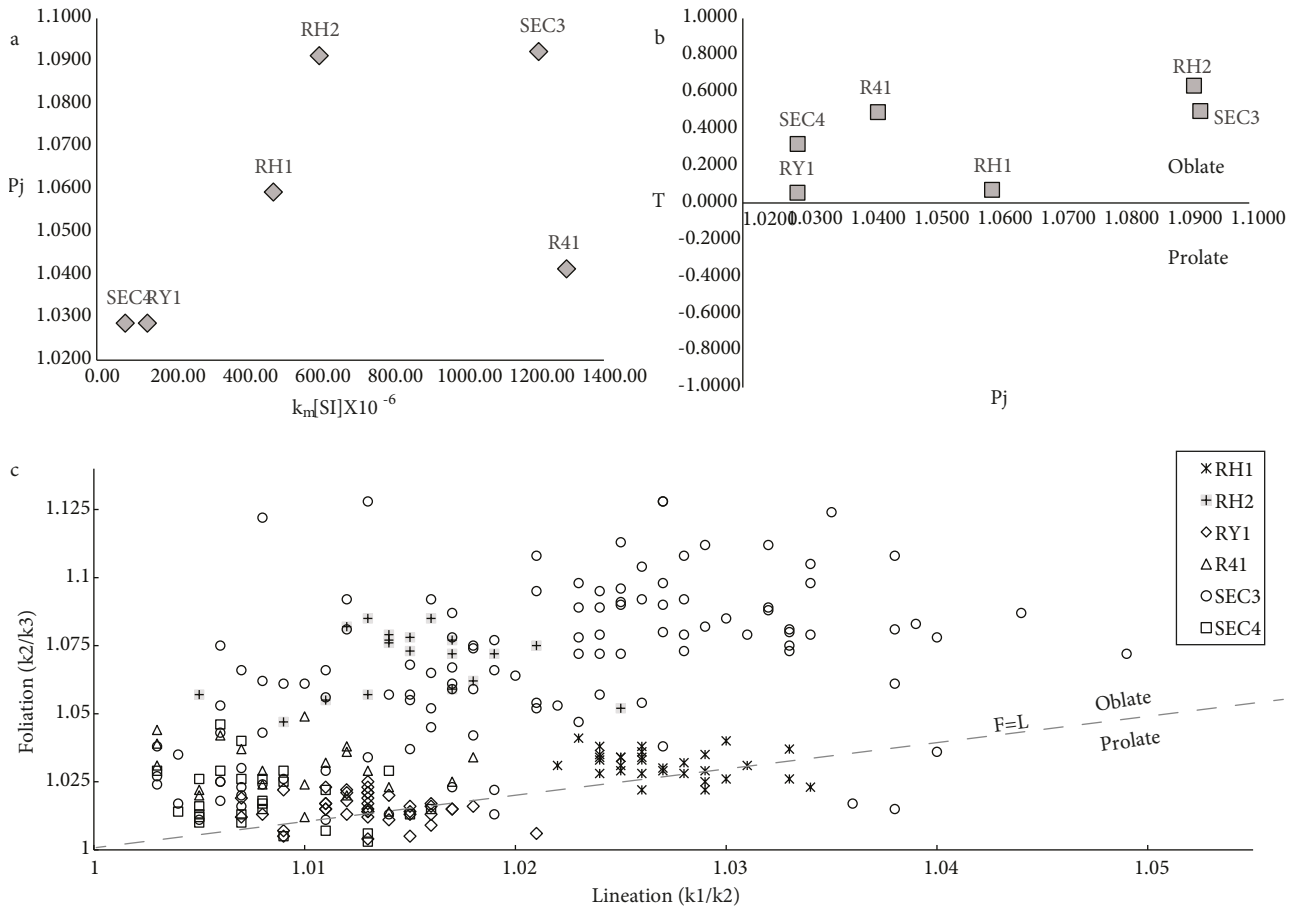


**Figure 4.** a) Plot of site mean corrected anisotropy degree ( $P_j$ ) versus site mean susceptibility ( $k_m$ ). b) Plot of site mean shape factor ( $T$ ) versus corrected anisotropy degree ( $P_j$ ). c) Flinn diagram of foliation ( $F = k_2/k_3$ ) and lineation ( $L = k_1/k_2$ ) AMS values for individual specimens of six sites. Site ellipsoid shapes vary from distinctly oblate to prolate.

The shape of the anisotropy ellipsoids is predominantly oblate, ranging from neutral ( $T \sim 0$  and  $L/F \sim 1$ ; RY1 and RH1) and moderately to strongly oblate ( $T > 0$  and  $F > L$ ; SEC4, SEC3 to R41, RH2, respectively) (Table; Figure 4b). Such a variation was described by Borradaile and Henry (1997) and Pares et al. (1999) as a result of increasing deformation. Although there is no site mean value showing a prolate AMS ellipsoid (Figure 4b), results from some sites (especially RY1 and RH1) have small percentages of prolate shape (Figure 4c).

The ellipsoids of all six AMS samples are moderate to well defined and have quite tight groups with small confidence ellipses (e). Particularly, the magnetic foliation ( $F$ ) shows a very clear cluster around the  $k_3$  axis with confidence ellipses e3 always lower (lower than  $\sim 10^\circ$ , except from one site R41 that shows  $\sim 15^\circ$ ; Table). The clustering of magnetic lineation  $L$ , similar to the low magnetic foliation dispersion  $k_1$  and  $k_2$  axes, is characterized by relatively low confidence ellipses e1 and e2 (lower than  $\sim 25^\circ$ ), with slightly higher values up to  $\sim 45^\circ$  at site R41 (Table).

According to all these parameters explained above and the distribution of the principal directions calculated from the six AMS ellipsoids, it is obvious that there is tectonic-related deformation overprinting the initial sedimentary depositional fabric. According to the formula given above, the calculated shortening values vary from a minimum of 18.36% at site RH1 to a maximum of 32.24% at site RH2 (Table).

#### 4.3. Balanced cross-sections

The results of the balanced sections and shortening ratio calculations are given in Figure 5. The shortening ratio calculations conducted on five balanced cross-sections differ between 22.4% and 28.9%. Although the maximum ratios are found at the center of the Haymana Anticline (between 25.1% and 28.9%, along sections B and C), the main trend shows that the shortening ratios decrease towards the eastern edge of the anticline, being 22.4% (along section D). Balanced cross-section studies also allow us to find the erosion amount in the Haymana

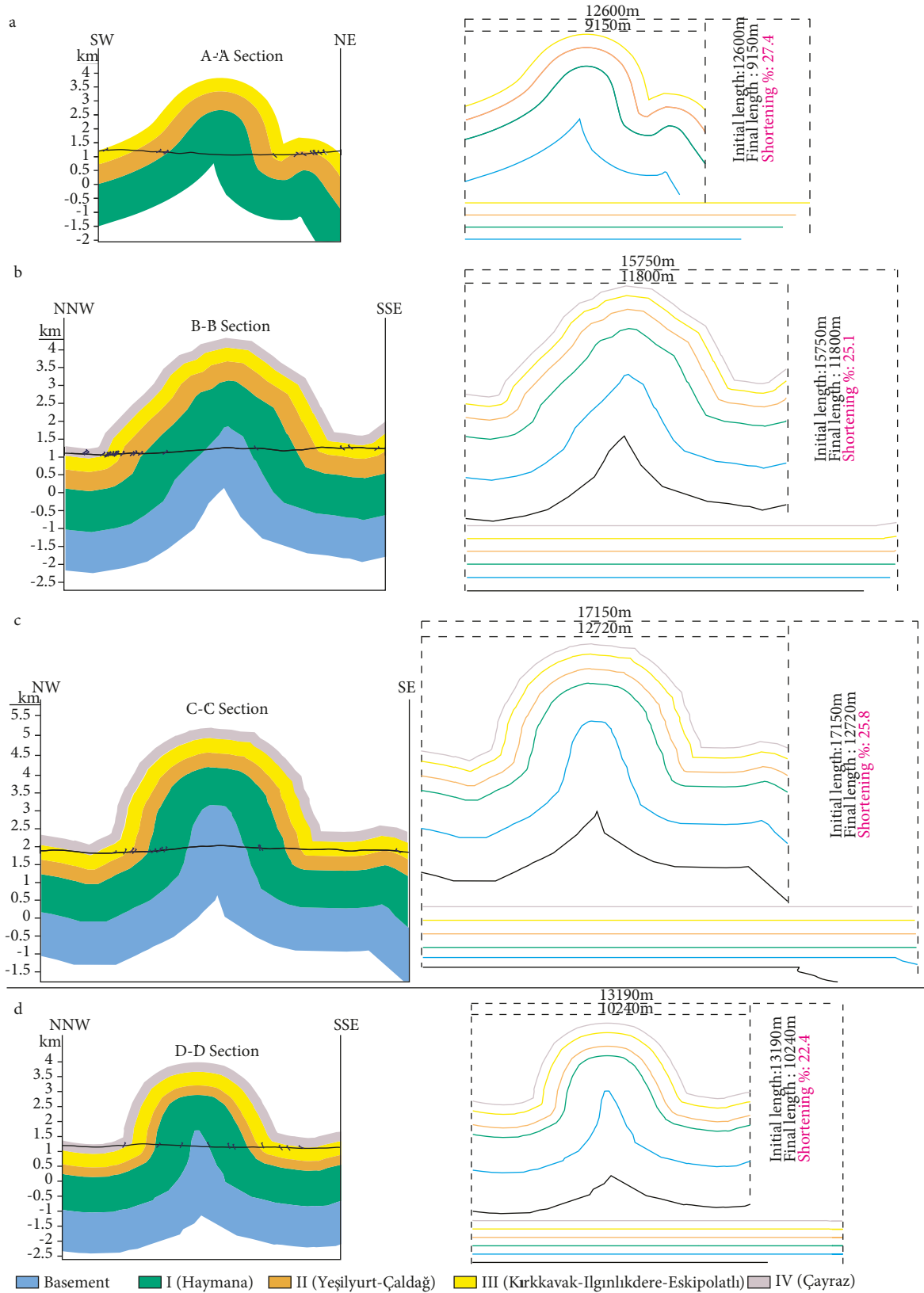


**Figure 5.** Balanced cross-sections of the Haymana Anticline and their structural-stratigraphic restorations showing shortening ratios. Cross-section orientations are given in Figure 2.

Anticline, which is greater than 3.5 km, and calculate the total true thickness of the sedimentary units as at least 4 km.

## 5. Discussion

### 5.1. Origin of magnetic susceptibility and AMS-based shortening calculations

The relationship between the AMS magnetofabric results and rock magnetics is a subject that has been investigated for a long time. The main purpose is to define any correlation between the tectonic deformation and the magnetofabric design and finally determine an empirical formula correlating magnetofabrics with the strain accumulated in deformed sedimentary strata. At the end, the obtained results allow us to obtain independent datasets that are comparable with the other structural evidence. However, due to the nature of the AMS methodology, the results might be influenced by a combination of many factors, the best known of which are the shape alignment of magnetofabric grains, the earth's gravity and magnetic fields, hydrodynamic effects, compaction, metamorphism, and stress-induced anisotropy due to tectonic origin (syn- and postdepositional) (Hrouda, 1982; Borradaile, 1988; Rochette et al., 1992). In this study, the site mean susceptibility ( $k_m$ ) in the six sites was found in an interval varying between  $\sim 50$  and  $1400 \times 10^{-6}$  (SI), which implies an independent distribution of the magnetofabric mineral content. Also, the AMS lineaments in each site were checked and gave almost  $90^\circ$  discrepancy from the true magnetic north-south directions, meaning that the earth's magnetic field effect is not worth considering (Figure 6). Since the sampled lithology represents a turbiditic succession with fine-grained/nonlaminated sedimentary levels, grain shape (due to gravitational field) and water current factors can be considered as low probability effects. Sedimentary rocks acquire their primary magnetic anisotropy during depositional diagenetic and sedimentary compaction (Sagnotti et al., 1998, 1999; Pares et al., 1999; Cifelli et al., 2004, 2005; Soto et al., 2009). In this phase, magnetic foliation ( $k_3$ , vertical) is very well defined and parallel to the sedimentation plane; however, magnetic lineations ( $k_1$  and  $k_2$ ) do not cluster but rather disperse within the magnetic plane. In our results, however, the  $k_3$  axis is almost vertical and  $k_1$  and  $k_2$  show moderate to good clustering. Due to the results of the AMS parameter outcomes, diagrams, and shapes of the AMS ellipsoids, we consider that the magnetofabric designs reveal a tectonic load-related deformation phase overprinting the sedimentary fabrics to tectonic ones during or after sedimentation (Figure 6). Depending on the magnetofabric deformation of magnetic minerals, it is very important to distinguish the tectonic effect on the samples (during or after sedimentation) from the compaction effect, which is formed by sedimentation

(Graham, 1966; Kligfield et al., 1981; Hrouda, 1982, 1993; Borradaile, 1988; Lowrie, 1989; Borradaile and Henry, 1997; Borradaile and Jackson, 2004), so it is possible to explain the tectonic deformation processes that reigned in the region.

According to the implemented experimental studies and their applications in the field, there are two types of magnetofabric patterns: 1) in the low deformation region by a compressional tectonic regime, the magnetic anisotropy lineations ( $k_1$ ) show a perpendicular tendency to the shortening directions ( $k_1$  parallel to the fold axis, bedding strike and  $k_3$  axis parallel to shortening direction) (Sagnotti et al., 1994; Borradaile and Henry, 1997; Kissel et al., 1997; Mattei et al., 1997; Pares et al., 1999; Soto et al., 2009); 2) for the rocks under extensional tectonic regimes, the magnetofabric design is tectonically controlled and maximum susceptibility vectors align subparallel to the local bedding dip directions (Mattei et al., 1997, 1999) or perpendicular to the main normal faults (Cifelli et al., 2005). In this regard, our results obviously indicate compressional setting-related deformation because in this study all  $k_1$  directions are parallel to the fold axis and the bedding strikes, and also all  $k_3$  axes are parallel to the shortening direction (Figure 7). Since it is known that the obtained AMS results are largely due to tectonic deformation, the shortening of this deformation can easily be calculated by the AMS method. The resulting calculation parameters have already been tested in a similar lithology and all samples were taken from the same lithology, so the reliability of the results is confirmed.

### 5.2. Correlation between magnetic fabric and geologically balanced cross-sections of the Haymana Anticline

Although the magnetofabric characteristic of the Haymana Formation is independent of the position of the sampling sites within the Haymana Anticline, the maximum shortening values are relatively higher at the center (up to 28.1%–32.2%) and the western sides of the anticline (except site RY1, which has 18.4%); however, they decrease gradually down to 18.3% towards the east (Table; Figure 7). This strain difference within the anticline is also supported by the restorations of the balanced cross-sections by 28.6% and 27.4% values calculated at the center and western edge, respectively, and 22.4% at the east.

The decrease in shortening ratios might be explained by oblique shortening, which generally occurs in the basins due to oblique collisions or subsequent transpressional deformations that mainly result from oblique indentations (Allen et al., 2003; McClay et al., 2004; Pérez-Cáceres et al., 2016).

The AMS based and restoration-based shortening ratio results are very similar. This implies that AMS-based shortening ratio calculations might be used for the folds for which visible strain markers are not enough to calculate

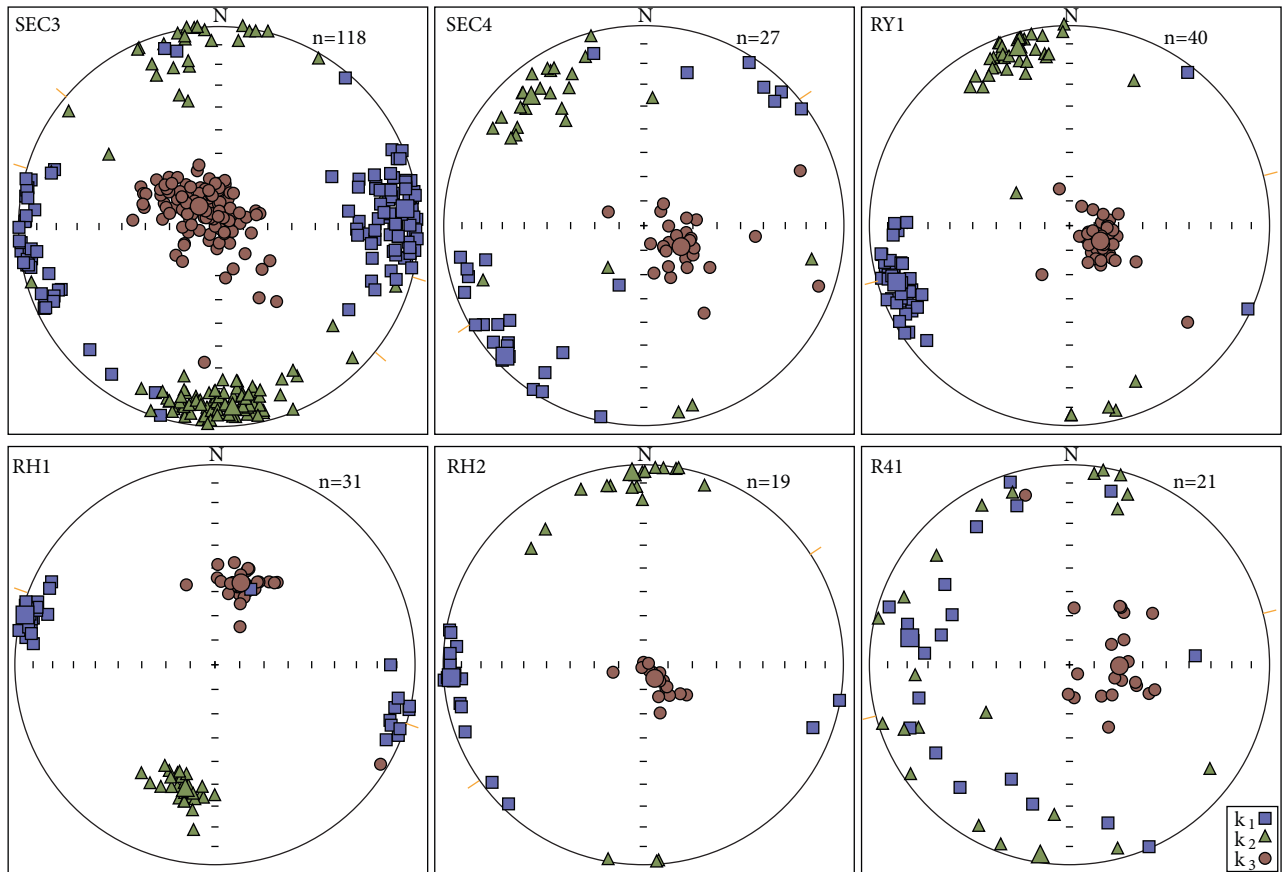


**Figure 6.** Lower hemisphere Schmidt equal area projection of the principal axes ( $k_1$ ,  $k_2$ , and  $k_3$ ) of the six AMS ellipsoids (bedding corrected) and their mean values (larger symbols) from six samples sites. Measured bedding strikes are shown orange dashes.

shortening ratios. In this study, although we mainly focus on the Haymana Anticline, we construct an extra balanced cross-section cutting the anticline and other elements in the basin. For this cross-section, we made a restoration and found a 28.9% shortening ratio (Figure 8). This result is also similar to the results obtained by AMS calculations and the other results proposed for the entire basin (Gülyüz, 2015). This implies that the AMS-based shortening ratio calculations are not only effective in local scale; they might also be useful in regional scale studies.

### 5.3. Implications for the regional tectonics

Central Anatolia has been shaped under a north-south contractional regime due to subduction of the Neo-Tethys Ocean and subsequent collision of intervening continental blocks during the Late Cretaceous to Late Paleogene, and the transcurrent tectonic regime has been the dominant deformation factor since the Late Neogene (Şengör et al., 1980; Koçyiğit, 1991; Okay et al., 1998, 2006, 2008; Bozkurt, 2001; Dilek, 2006; Kaymakçı et al., 2009; Pourteau et al., 2010, 2013; Gürer et al., 2016; van Hinsbergen et al., 2016). The effects of both contractional and transcurrent tectonic regimes give way to counterclockwise vertical

block rotations in the Kırşehir Block since the Cretaceous time (Sanver and Ponat, 1981; McClusky et al., 2000) and there is geophysical evidence for the same sense rotations for the Neogene period (Büyüksaraç, 2007; Aydemir, 2011). The Neogene counterclockwise rotations in Central Anatolia are solely related to the convergence between the Arabian and Anatolian plates resulting in westward escape of the Anatolian plate along the North and East Anatolian Fault zones (e.g., Büyüksaraç, 2007; Piper et al., 2010). Additionally, for Central Anatolia, an indentation (south to north) of the Kırşehir Block into the Pontides during the Eocene to Miocene was proposed in some recent studies (Meijers et al., 2010; Lefebvre et al., 2013). Also, the traces of the indentation in the Haymana Basin are explained by a model indicating that the Dereköy Thrust Fault with left-lateral sense defined as a basin bounding fault is the western extension of the Hirfanlar-Hacı Bektaş fault zone dissecting the Kırşehir Block into two segments (Lefebvre et al., 2013), which is proposed as the main fault controlling the movement of the indenter, and that it accommodated the indentation-related deformation and transferred into the basin after or during the continental

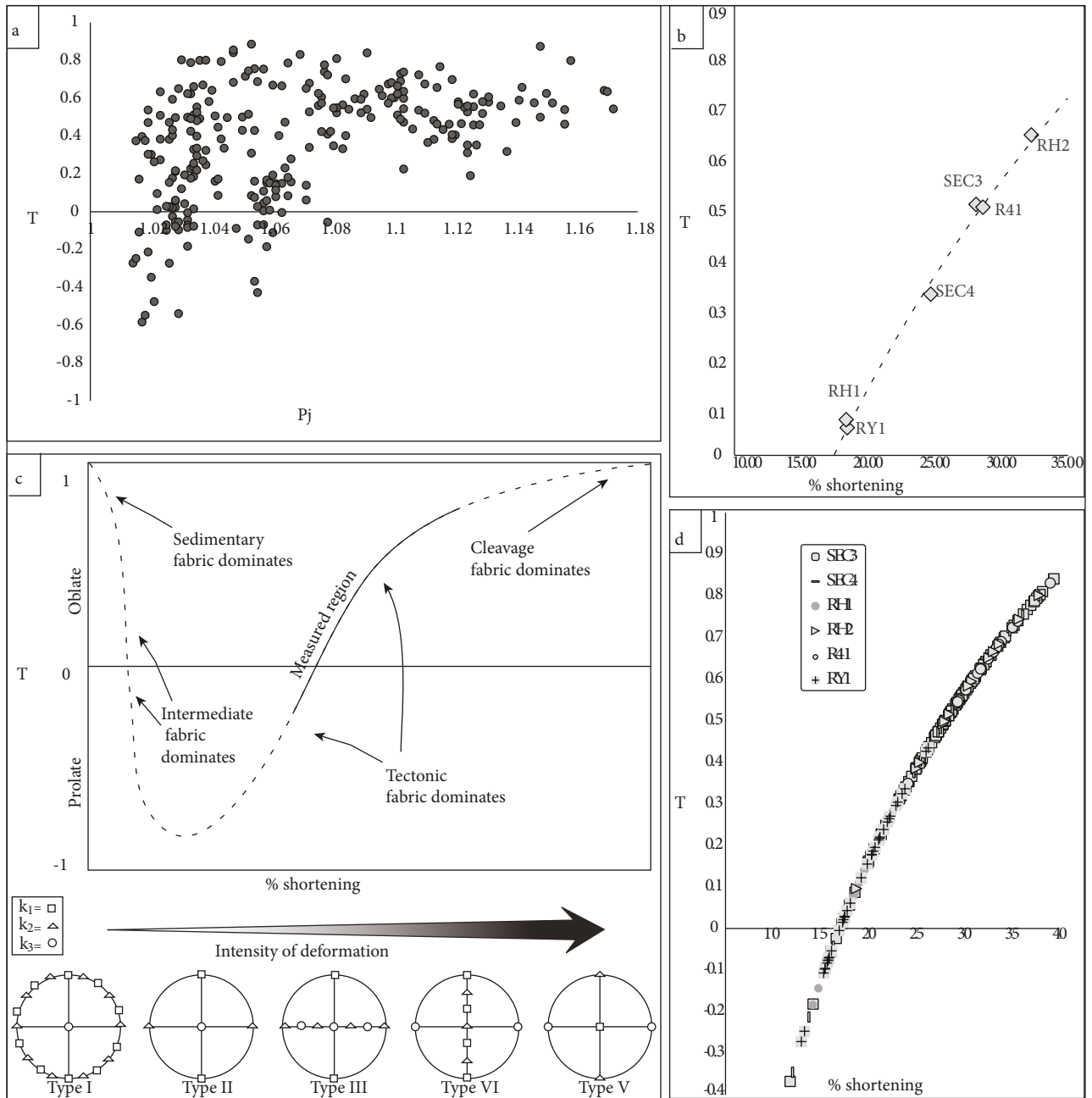


**Figure 7.** a) Diagram showing the variation of the corrected anisotropy degree ( $P_j$ ) against the shape parameter for whole measurements. b) Plot of shape parameter T versus % shortening site mean results. c) Conceptual model for evolution of AMS fabric in weakly to strongly deformed sedimentary rocks. Shape factor (T) versus % shortening results diagram compared to the typical trend expected from increasing intensity of deformation. Equal area lower hemisphere projections show idealized changes in AMS ellipsoid directions from sedimentary (Type I), sedimentary/tectonic (Type II-II-IV), and strong tectonic fabric. d) Plot of shape parameter T versus % shortening from measured result.

collision occurring between the Pontides and Tauride Block (Gülyüz, 2015; Özkaptan, 2016).

According to the clustered shape of the susceptibility vectors and the other output diagrams, the six AMS ellipsoids are classified as ‘tectonic fabric’ or ‘deformation

fabric’. Therefore, these results must be closely associated with the effect of deformation that reigned in the region. The obtained AMS directions with the local bedding attitudes clearly show a compressive/transpressive origin, which is in accordance with surface structural evidences.

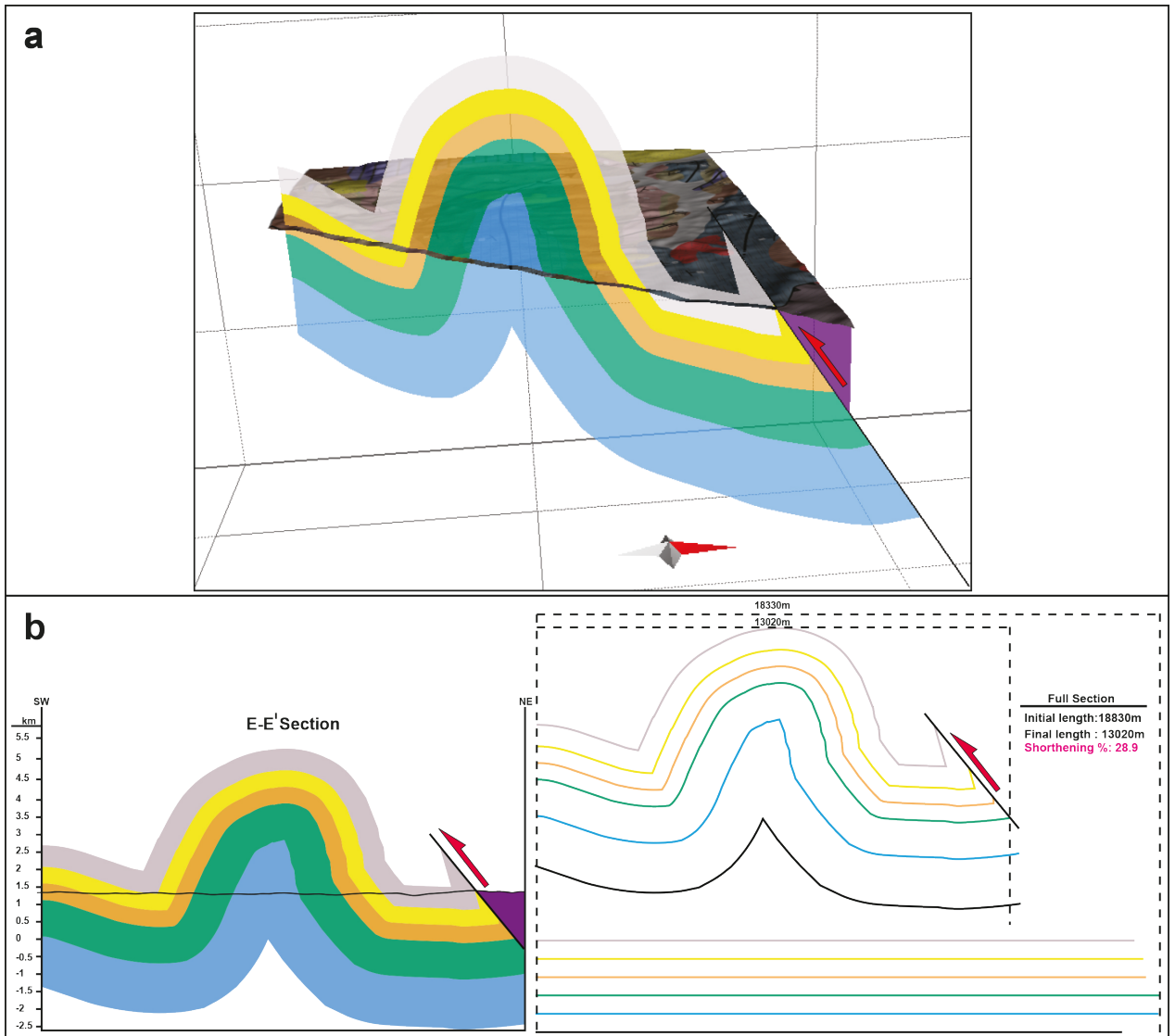


**Figure 8.** a) 3D view of balancing of geological cross-section (E-E') in Figure 2. b) Structural-stratigraphic restoration of the cross-section in the Haymana Anticline.

Hence, the minimum susceptibility axis ( $k_3$ ) of all sites is nearly normal to local bedding planes and the maximum susceptibility axis ( $k_1$ ) is perpendicular to the direction of the main shortening axis (~north to south), parallel to the Haymana Anticline fold axis (E-W) and the Dereköy Thrust Fault at the northern margin of the Haymana Basin.

Besides our quantitative AMS-based results, the compressional/transpressional tectonic setting and related strain differences in the basin were also checked by the balanced cross-sections and their restorations. This allowed to check the AMS-based results and prove compressional/transpressional-origin deformation for the basin. Although our results do not give any constraint about the timing of the compressional deformation, the studies of Özsayın and Dirik (2007, 2011), Kaymakçı et al.

(2009), Gülyüz (2015), and Özkaptan (2016) indicated that a compressional/transpressional setting resulted from the collision that occurred between the TAB and Pontides or from the oblique indentation of the KB into the Pontides, active in the region between the late Eocene to early Miocene. This time constraint indicates that our AMS results from the Late Cretaceous Haymana Formation are related to the postdepositional contractional deformation. The traces of these deformations are observed in our results as compressional/transpressional setting-related AMS patterns and a decrease in shortening ratios towards the east side of the Haymana Anticline. In this study, we propose that these local findings are associated with the collision between the TAB and the Pontides, allowing compressional deformation, and the syn- or syn- to

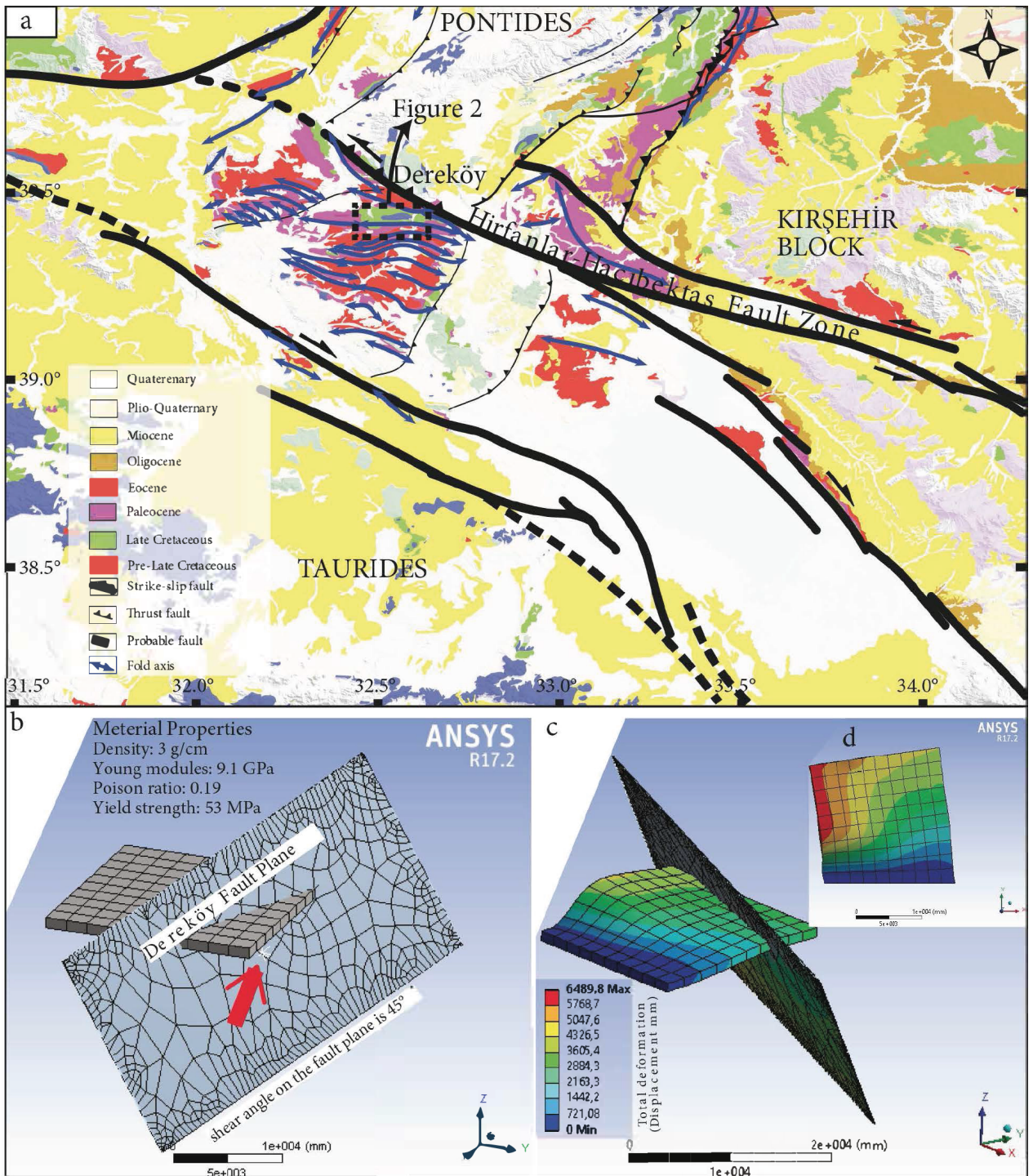


**Figure 9.** a) Geological map of Central Anatolia showing the elongation of the main structures. Westward extension of the Hirfanlar-Hacıbektaş Fault Zone corresponds to the Dereköy Thrust in the Haymana Basin (black rectangle). b) Inputs of ANSYS model (tentative) showing the initial geometries of the latterly deformed modeled rock volume, properties of which are close to claystone and carbonate rocks (the main components of the deformed layers) and the position of a thrust fault with left-lateral sense (proposing the Dereköy Fault Plane, as a rigid plane in the model). c) The 3D model showing the deformation distribution after the displacement of the proposed the Dereköy Fault Plane (54,000 mm along Z axis and -54,000 mm along X axis). d) The 2D view of the deformation distribution. Deformation increases towards the left (or west in the basin); dimensions on the model are in millimeters.

postcollisional oblique indentation of the KB into the Pontides (Lefebvre et al., 2013), allowing the activation of the Dereköy Thrust Fault as a left-lateral transpressional fault resulting in the differential shortening ratios of the Haymana Anticline (Figure 9). The reason behind the oblique indentation might be the segmentation of the Kırşehir Block along the NW-SE trending faults and differential movements/rotations of the microblocks, as discussed by Lefebvre et al. (2013). Our results may have signs of active transcurrents or wrench tectonics (e.g., Büyüksaraç, 2007; Piper et al., 2010), but we propose that the effects of the Neogene events are minor in the Haymana Formation while the dominant factor was the oblique indentation of the Kırşehir Block. In order to test the oblique indentation model, a tentative finite element model that was constructed using the R17.2 version of ANSYS software was used in the study. In this model, the Dereköy Thrust Fault was defined as a moving (along two directions, towards west and south) rigid body that creates deformation (displacement) on a modeled volume representing a claystone body (Figure 9). The results of the model clearly show that if the Dereköy Thrust Fault works as a reverse fault with sinistral sense, shortening ratios in the basin will decrease towards the west, as indicated in the AMS- and restoration-based shortening results of the study.

## 6. Conclusions

In this study, we conclude that the shapes of the AMS ellipsoids can be not only correlated in the direction of their eigenvectors ( $k_{1,2,3}$ ) but also utilized as strain markers to establish a quantitative indicator of the local to regional deformation history. Based on the results of both the paleomagnetic (AMS) and the other surface kinematic data from the Haymana Anticline in the Central Anatolia, we conclude that:

- Magnetic mineralogy analyses show that although each stratigraphic site/level has a different type of magnetic carriers, they all exhibit ferromagnetic characteristics

## References

- Allen MB, Ghassemi MR, Shahrabi M, Qorashi M (2003). Accommodation of late Cenozoic oblique shortening in the Alborz range, northern Iran. *J Struct Geol* 25: 659-672.
- Averbuch O, Frizon de Lamotte, D, Kissel C (1992). Magnetic fabric as a structural indicator of the deformation path within a fold-thrust structure: a test case from the Corbières (NE Pyrenees, France). *J Struct Geol* 14: 461-474.
- Aydemir A (2009). Tectonic investigation of Central Anatolia, Turkey, using geophysical data. *J Appl Geophys* 68: 321-334.
- Aydemir A (2011). An integrated geophysical investigation of Haymana Basin and hydrocarbon prospective Kirkkavak Formation in Central Anatolia, Turkey. *Petrol Geosci* 17: 91-100.
- Aydemir A, Ateş A (2006). Structural interpretation of the Tuzgözü and Haymana Basins, Central Anatolia, Turkey, using seismic, gravity and aeromagnetic data. *Earth Planets Space* 58: 951-961.
- Benn K (1994). Overprinting of magnetic fabrics in granites by small strains: numerical modelling. *Tectonophysics* 233: 153-162.
- that lead to determination of the deformation via magnetofabrics in each location.
- While the main magnetic susceptibility contribution from paramagnetism is to small percentage of ferromagnetic minerals to bulk susceptibility, the anisotropy degree varies rather than magnetic mineralogy but is highly related to the amount of deformation affected in the sampled matrix.
  - The Upper Cretaceous shale-mudstone successions of the sampled Haymana Anticline show well-developed, low-to-moderately deformed AMS susceptibility ellipsoids in 6 different levels.
  - The maximum susceptibility results of the Haymana Anticline are clearly consistent with the structural evidence so  $k_1$  is almost parallel to the fold axis trending ~E to W.
  - As a quantitative deformation indication, we followed the studies of Pares and van der Pluijm (2003, 2004) proposed for low-to-moderately deformed mudstone and we calculated an 18%–32% shortening ratio based on magnetic fabric in the area.
  - Four geologically balanced cross-section results throughout the Haymana Anticline indicate ~22%–28% maximum shortening ratio, so the two independent datasets have a close correlation, indicating the possibility of using AMS-based shortening calculations in sedimentary basins in which kinematic indicators are not enough to calculate shortening ratios.
  - Since there are many factors affecting the correlation between tectonic strain and AMS deformation fabric, applying the AMS-based shortening calculation method for other lithologies (except mudstones) requires detailed step-wise analyses/experiments.

## Acknowledgments

We would like to thank Dr Nilay Gülyüz for her help with English editing. We are grateful to Dr Burak Taymuş for his contribution in modeling in Figure 9. We are also grateful to Aydın Büyüksaraç and two anonymous reviewers for their very constructive comments, which helped to considerably improve the original manuscript.



- Bilim, F, Ateş A (2007). Identifying block rotations from remanent magnetization effect: example from northern Central Turkey. *Earth Planets Space* 59: 33-38.
- Bilim F, Aydemir A, Ateş A (2015). Determination of block rotations and the Curie Point Depths of magnetic sources along the NW–SE-trending Sülüklü-Cihanbeyli-Gölören and Şereflikoçhisar-Aksaray Fault Zones, Central Anatolia, Turkey. *Geodin Acta* 27: 203-13.
- Borradaile GJ (1987). Anisotropy of magnetic susceptibility: rock composition versus strain. *Tectonophysics* 138: 327-329.
- Borradaile GJ (1988). Magnetic susceptibility, petrofabrics and strain. *Tectonophysics* 156: 1-20.
- Borradaile GJ (1991). Correlation of strain with anisotropy of magnetic-susceptibility (AMS). *Pure Appl Geophys* 135: 15-29.
- Borradaile GJ, Jackson M (2004). Anisotropy of magnetic susceptibility (AMS): magnetic petrofabrics of deformed rocks. *Geol Soc Sp* 238: 299-360.
- Borradaile GJ, Jackson M (2010). Structural geology, petrofabrics and magnetic fabrics (AMS, AARM, AIRM). *J Struct Geol* 32: 1519-1551.
- Borradaile GJ, Mothersill J, Tarling D, Alford C (1986). Sources of magnetic susceptibility in a slate. *Earth Planet Sc Lett* 76: 336-340.
- Borradaile G, Tarling DH (1981). The influence of deformation mechanisms on magnetic fabrics in weakly deformed rocks. *Tectonophysics* 77: 151-168.
- Bozkurt E (2001). Neotectonics of Turkey - a synthesis. *Geodin Acta* 14: 3-30.
- Büyüksaraç A (2007). Investigation into the regional wrench tectonics of inner East Anatolia (Turkey) using potential field data. *Phys Earth Planet In* 160: 86-95.
- Büyüksaraç A, Jordanova D, Ateş A, Karloukovski V (2005). Interpretation of the gravity and magnetic anomalies of the Cappadocia Region, Central Turkey. *Pure Appl Geophys* 162: 2197-2213.
- Chadima, M, Jelinek V (2009). AniSoft 4.2: Anisotropy Data Browser for Windows. Brno, Czech Republic: AGICO Inc.
- Cifelli F, Mattei M, Chadima M, Hirt AM, Hansen A (2005). The origin of tectonic lineation in extensional basins: Combined neutron texture and magnetic analyses on “undeformed” clays. *Earth Planet Sc Lett* 235: 62-78.
- Cifelli F, Mattei M, Hirt AM, Günther A (2004). The origin of tectonic fabrics in “undeformed” clays: the early stages of deformation in extensional sedimentary basins. *Geophys Res Lett* 31: 2-5.
- Çinku MC (2017). Paleomagnetic results from Northeast Anatolia: remagnetization in Late Cretaceous sandstones and tectonic rotation at the Eastern extension of the Izmir–Ankara–Erzincan suture zone. *Acta Geophys* 65: 1095-1109.
- Çinku MC, Hisarlı ZM, Yılmaz Y, Ülker B, Kaya N, Öksüm E, Orbay N, Özbey ZÜ (2016). The tectonic history of the Niğde-Kırşehir Massif and the Taurides since the Late Mesozoic: Paleomagnetic evidence for two-phase orogenic curvature in Central Anatolia. *Tectonics* 35: 772-811.
- Collinson DW, editor (1983). *Methods in Rock Magnetism and Palaeomagnetism. Paleomagnetism-Techniques and Instrumentation*. 1st ed. London, UK: Springer Science & Business Media.
- Cox A, Doell RR (1960). Review of paleomagnetism. *Geol Soc Am Bull* 71: 645-768.
- Dahlstrom CDA (1969). Balanced cross sections. *Can J Earth Sci* 6: 743-757.
- Dilek Y (2006). Collision tectonics of the Mediterranean region: causes and consequences. *Geol S Am S* 409: 1-14.
- Evans MA, Lewchuk MT, Elmore RD (2003). Strain partitioning of deformation mechanisms in limestones: examining the relationship of strain and anisotropy of magnetic susceptibility (AMS). *J Struct Geol* 25: 1525-1549.
- Fabian K, Shcherbakov VP, McEnroe SA (2013). Measuring the Curie temperature. *Geochem Geophys Geosy* 14: 947-961.
- Görür N, Oktay FY, Seymen I, Şengör AMC (1984). Palaeotectonic evolution of the Tuzgölü basin complex, Central Turkey: sedimentary record of a Neo-Tethyan closure. *Geol Soc Sp* 17: 467-482.
- Görür N, Tüysüz O, Şengör AMC (1998). Tectonic evolution of the Central Anatolian basins. *Int Geol Rev* 40: 831-850.
- Gülyüz E (2015). Tectono-stratigraphic and thermal evolution of the Haymana Basin, Central Anatolia, Turkey. PhD, Middle East Technical University, Ankara, Turkey.
- Gürer D, Hinsbergen DJJ, Matenco L, Corfu F, Cascella A (2016). Kinematics of a former oceanic plate of the Neotethys revealed by deformation in the Ulukışla basin (Turkey). *Tectonics* 35: 2385-2416.
- Hirt AM, Evans KE, Engelder T (1995). Correlation between magnetic anisotropy and fabric for Devonian shales on the Appalachian Plateau. *Tectonophysics* 247: 121-132.
- Hisarlı ZM, Çinku MC, Ustaömer T, Keskin M, Orbay N (2016). Neotectonic deformation in the Eurasia–Arabia collision zone, the East Anatolian Plateau, E Turkey: evidence from palaeomagnetic study of Neogene–Quaternary volcanic rocks. *Int J Earth Sci* 105: 139-65.
- Housen BA, Kanamatsu T (2003). Magnetic fabrics from the Costa Rica margin: sediment deformation during the initial dewatering and underplating process. *Earth Planet Sc Lett* 206: 215-228.
- Housen BA, Richter C, van der Pluijm BA (1993). Composite magnetic anisotropy fabrics: experiments, numerical models and implications for the quantification of rock fabrics. *Tectonophysics* 220: 1-12.
- Housen BA, van der Pluijm BA (1991). Slaty cleavage development and magnetic anisotropy fabrics. *J Geophys Res* 96: 9937-9946.
- Hrouda F (1982). Magnetic anisotropy of rocks and its application in geology and geophysics. *Geophys Surv* 5: 37-82.
- Hrouda F (1991). Models of magnetic anisotropy variations in sedimentary thrust sheets. *Tectonophysics* 185: 203-210.
- Hrouda F (1993). Theoretical models of magnetic anisotropy to strain relationship revisited. *Phys Earth Planet In* 77: 237-249.

- Hrouda F, Janak F (1976). The changes in shape of the magnetic susceptibility ellipsoid during progressive metamorphism and deformation. *Tectonophysics* 34: 135-148.
- Hrouda F, Krejci O, Potfaj M, Stranik Z (2009). Magnetic fabric and weak deformation in sandstones of accretionary prisms of the Flysch and Klippen Belts of the Western Carpathians: mostly offscraping indicated. *Tectonophysics* 479: 254-270.
- Huang W, Dupont-Nivet G, Lippert PC, van Hinsbergen DJJ, Hallot E (2013). Inclination shallowing in Eocene Linzizong sedimentary rocks from southern Tibet: correction, possible causes and implications for reconstructing the India-Asia collision. *Geophys J Int* 194: 1390-1411.
- Jelinek V, editor (1977). *The Statistical Theory of Measuring Anisotropy of Magnetic Susceptibility of Rocks and Its Application*. 1st ed. Brno, Czechoslovakia: Geofyzika Brno.
- Jelinek V (1978). Statistical processing of magnetic susceptibility measured on groups of specimens. *Stud Geophys Geod* 22: 50-62.
- Jelinek V (1981). Characterization of the magnetic fabric of rocks. *Tectonophysics* 79: 63-67.
- Kaymakçı N, Özçelik Y, White SH, Van Dijk PM (2009). Tectonostratigraphy of the Çankırı Basin: late Cretaceous to early Miocene evolution of the Neotethyan suture zone in Turkey. *Geol Soc Sp* 311: 67-106.
- Ketin I (1966). Tectonic units of Anatolia (Asia Minor). *Min Res Exp Bull* 66: 23-34.
- Kissel C, Laj C, Lehman B, Labyrie L, Bout-Roumazeilles V (1997). Changes in the strength of the Iceland-Scotland Overflow Water in the last 200,000 years: evidence from magnetic anisotropy analysis of core SU90-33. *Earth Planet Sc Lett* 152: 25-36.
- Kissel C, Laj C, Poisson A, Savascin Y, Simeakis K, Mercier, JL (1986). Paleomagnetic evidence for Neogene rotational deformations in the Aegean domain. *Tectonics* 5: 783-796.
- Koçyiğit A (1991). An example of an accretionary forearc basin from northern Central Anatolia and its implications for the history of subduction of Neo-Tethys in Turkey. *Geol Soc Am Bull* 103: 22-36.
- Lefebvre C, Meijers MJM, Kaymakçı N, Peynircioğlu A, Langereis CG, van Hinsbergen DJJ (2013). Reconstructing the geometry of central Anatolia during the late Cretaceous: large-scale Cenozoic rotations and deformation between the Pontides and Taurides. *Earth Planet Sc Lett* 366: 83-98.
- Lowrie W (1989). Magnetic analysis of rock fabric. In: James DE, editor. *Encyclopedia of Solid Earth Geophysics*. 1st ed. Boston, MA, USA: Springer, pp. 698-706.
- Mattei M, Sagnotti L, Faccenna C, Funicello R (1997). Magnetic fabric of weakly deformed clay-rich sediments in the Italian peninsula: relationship with compressional and extensional tectonics. *Tectonophysics* 271: 107-122.
- Mattei M, Speranza F, Argentieri A, Rossetti F, Sagnotti L, Funicello R (1999). Extensional tectonics in the Amantea basin (Calabria, Italy): a comparison between structural and magnetic anisotropy data. *Tectonophysics* 307: 33-49.
- McClay KR, Whitehouse PS, Dooley, T, Richards M (2004). 3D evolution of fold and thrust belts formed by oblique convergence. *Mar Petrol Geol* 21: 857-877.
- McClusky S, Balassanian S, Barka A, Demir C, Ergintav S, Georgiev I, Gurkan O, Hamburger M, Hurst K, Kahle H et al. (2000). GPS constraints on plate motion and deformation in the eastern Mediterranean: implications for plate dynamics. *J Geophys Res* 105: 5695-5719.
- Meijers MJM, Kaymakçı N, Van Hinsbergen DJJ, Langereis CG, Stephenson RA, Hippolyte J (2010). Late Cretaceous to Paleocene oroclinal bending in the central Pontides (Turkey). *Tectonics* 29: 1-21.
- MTA (2002). *Geological Map of Turkey (Scale 1:500,000)*. Ankara, Turkey: General Directorate of Mineral Research and Exploration of Turkey (MTA).
- Mullender TAT, Van Velzen AJ, Dekkers MJ (1993). Continuous drift correction and separate identification of ferrimagnetic and paramagnetic contribution in thermomagnetic runs. *Geophys J Int* 114: 663-672.
- Nairn SP, Robertson AHF, Ünlügenç UC., Tasli K, İnan N (2013). Tectonostratigraphic evolution of the Upper Cretaceous-Cenozoic central Anatolian basins: an integrated study of diachronous ocean basin closure and continental collision. *Geol Soc Sp* 372: 343-384.
- Noltimier HC (1971). Magnetic rock cylinders with negligible shape anisotropy. *J Geophys Res* 76: 4035-4037.
- Okay AI (2008). *Geology of Turkey: a synopsis*. *Anschchnitt* 21: 19-42.
- Okay AI, Altiner D (2016). Carbonate sedimentation in an extensional active margin: Cretaceous history of the Haymana region, Pontides. *Int J Earth Sci* 105: 2013-2030.
- Okay AI, Harris NBW, Kelley SP (1998). Exhumation of blueschists along a Tethyan suture in northwest Turkey. *Tectonophysics* 285: 275-299.
- Okay AI, Tüysüz O, Satır M, Özkan-Altın S, Altın D, Sherlock S, Eren RH (2006). Cretaceous and Triassic subduction-accretion, HP/LT metamorphism and continental growth in the Central Pontides, Turkey. *Geol Soc Am Bull* 118: 1247-1269.
- Oliva-Urcia B, Rahl JM, Schleicher AM, Pares JM (2010). Correlation between the anisotropy of the magnetic susceptibility, strain and X-ray texture goniometry in phyllites from Crete, Greece. *Tectonophysics* 486: 120-131.
- Owens WH (1974). Mathematical model studies on factors affecting the magnetic anisotropy of deformed rocks. *Tectonophysics* 24: 115-131.
- Özkaptan M (2016). Post-Late Cretaceous rotational evolution of Neotethyan sutures around Ankara Region. PhD, Middle East Technical University, Ankara, Turkey.
- Özkaptan, M, Kaymakçı, N, Langereis CG, Gülyüz, E, Özacar A, Uzel B, Sözbilir H (2018). Age and kinematics of the Burdur Basin: Inferences for the existence of the Fethiye Burdur Fault Zone in SW Anatolia (Turkey). *Tectonophysics* 744: 256-274.
- Özsayın E, Dirik K (2007). Quaternary activity of the Cihanbeyli and Yeniceoba Fault Zones: İnonu-Eskişehir Fault System, Central Anatolia. *Turk J Earth Sci* 16: 471-492.

- Özsayın E, Dirik K (2011). The role of oroclinal bending in the structural evolution of the Central Anatolian Plateau: evidence of a regional changeover from shortening to extension. *Geol Carpath* 62: 345-359.
- Pares JM, van der Pluijm BA (2002). Phyllosilicate fabric characterization by low-temperature anisotropy of magnetic susceptibility (LT-AMS). *Geophys Res Lett* 29: 68.
- Pares JM, van der Pluijm BA (2003). Magnetic fabrics and strain in pencil structures of the Knobs Formation, Valley and Ridge Province, US Appalachians. *J Struct Geol* 25: 1349-1358.
- Pares JM, van der Pluijm BA (2004). Correlating magnetic fabrics with finite strain: Comparing results from mudrocks in the Variscan and Appalachian Orogens. *Geol Acta* 2: 213-220.
- Pares JM, van der Pluijm BA, Dinares-Turell J (1999). Evolution of magnetic fabrics during incipient deformation of mudrocks (Pyrenees, northern Spain). *Tectonophysics* 307: 1-14.
- Passier HF, de Lange GJ, Dekkers MJ (2001). Magnetic properties and geochemistry of the active oxidation front and the youngest sapropel in the eastern Mediterranean sea. *Geophys J Int.* 145: 604-614.
- Perez-Caceres I, Simancas JF, Martinez Poyatos D, Azor A, Gonzalez Lodeiro F (2016). Oblique collision and deformation partitioning in the SW Iberian Variscides. *Solid Earth* 7: 857-872.
- Piper JD, Gürsoy H, Tatar O, Beck ME, Rao A, Koçbulut F, Mesci BL (2010). Distributed neotectonic deformation in the Anatolides of Turkey: a palaeomagnetic analysis. *Tectonophysics* 488: 31-50.
- Pourteau A, Candan, O, Oberhansli R (2010). High-pressure metasediments in central Turkey: constraints on the Neotethyan closure history. *Tectonics* 29: 1-18.
- Pourteau A, Sudo M, Candan O, Lanari P, Vidal O, Oberhansli R (2013). Neotethys closure history of Anatolia: insights from 40Ar-39Ar geochronology and P-T estimation in high-pressure metasedimentary rocks. *J Metamorph Geol* 31: 585-606.
- Ramsay JG, editor (1967). *Folding and Fracturing of Rocks*. 1st ed. Caldwell, NJ, USA: Blackburn Press.
- Richter C (1992). Particle motion and the modelling of strain response in magnetic fabrics. *Geophys J Int* 110: 451-464.
- Robion P, Grelaud S, Frizon de Lamotte D (2007). Pre-folding magnetic fabrics in fold-and-thrust belts: why the apparent internal deformation of the sedimentary rocks from the Minervois basin (NE - Pyrenees, France) is so high compared to the Potwar basin (SW - Himalaya, Pakistan)? *Sediment Geol* 196: 181-200.
- Rochette P (1987). Magnetic susceptibility of the rock matrix related to magnetic fabric studies. *J Struct Geol* 9: 1015-1020.
- Rochette P, Jackson M, Aubourg C (1992). Rock magnetism and the interpretation of anisotropy of magnetic susceptibility. *Rev Geophys* 30: 209-226.
- Rojay B (2013). Tectonic evolution of the Cretaceous Ankara Ophiolitic Mélange during the Late Cretaceous to pre-Miocene interval in Central Anatolia, Turkey. *J Geodyn* 65: 66-81.
- Sagnotti L, Faccenna C, Funicello R, Mattei M (1994). Magnetic fabric and structural setting of Plio-Pleistocene clayey units in an extensional regime: the Tyrrhenian margin of central Italy. *J Struct Geol* 16: 1243-1257.
- Sagnotti L, Mattei M, Faccenna C, Funicello R (1994). Paleomagnetic evidence for no tectonic rotation of the central Italy Tyrrhenian Margin since Upper Pliocene. *Geophys Res Lett* 21: 481-484.
- Sagnotti L, Speranza F, Winkler A, Mattei M, Funicello R (1998). Magnetic fabric of clay sediments from the external northern Apennines (Italy). *Phys Earth Planet Int* 105: 73-93.
- Sagnotti L, Winkler A, Montone P, Di Bella L, Florindo F, Mariucci MT, Frepoli A (1999). Magnetic anisotropy of Plio-Pleistocene sediments from the Adriatic margin of the northern Apennines (Italy): implications for the time-space evolution of the stress field. *Tectonophysics* 311: 139-153.
- Sanver, M, Ponat E (1981). Kırşehir ve dolaylarına ilişkin paleomanyetik bulgular, Kırşehir Masifinin rotasyonu. *İstanbul Yerbilimleri* 2: 231-238 (in Turkish).
- Scriba H, Heller F (1978). Measurements of anisotropy of magnetic susceptibility using inductive magnetometers. *J Geophys* 44: 341-352.
- Şengör AMC, Yılmaz Y (1981). Tethyan evolution of Turkey: a plate tectonic approach. *Tectonophysics* 75: 181-241.
- Şengör AMC, Yılmaz Y, Ketin I (1980). Remnants of a pre-Late Jurassic ocean in northern Turkey: fragments of Permian-Triassic Paleotethys? *Geol Soc Am Bull* 91: 599-609.
- Soto R, Larrasoana JC, Arlegui LE, Beamud E, Oliva-Urcia B, Simon JL (2009). Reliability of magnetic fabric of weakly deformed mudrocks as a palaeostress indicator in compressive settings. *J Struct Geol* 31: 512-522.
- Tarling DH, Hrouda F, editors (1993). *The Magnetic Anisotropy of Rocks*. 1st ed. London, UK: Chapman and Hall.
- Tripathy NR (2009). Degree of magnetic anisotropy as a strain-intensity gauge in a saturated finite-strain zone. *J Geol Soc London* 166: 9-12.
- Ünalın G, Yüksel V, Tekeli T, Gönenç O, Seyirt Z, Hüseyin S (1976). The stratigraphy and palaeogeographical evolution of the Upper Cretaceous-Lower Tertiary sediments in the Haymana-Polatlı region (SW of Ankara). *Bulletin of the Geological Society of Turkey* 19: 159-176.
- Uygun A (1981). Tuz Gölü havzasının jeolojisi, evaporit, oluşumları ve hidrokarbon olanakları. In: Doğan P, editor. 35th Scientific and Technical Congress of the Geological Society of Turkey. Central Anatolia Geology Symposium Proceedings, pp. 68-71 (in Turkish).
- van Hinsbergen DJJ, Maffione M, Plunder A, Kaymakçı N, Ganerod M, Hendriks BWH, Peters K (2016). Tectonic evolution and paleogeography of the Kırşehir Block and the Central Anatolian Ophiolites, Turkey. *Tectonics* 35: 983-1014.
- Woodcock NH (1977). Specification of fabric shapes using an eigenvalue method. *Bull Geol Soc Am* 88: 1231-1236.
- Yüksel S (1970). Etude géologique de la région d'Haymana (Turquie Centrale). PhD, l'Université de Nancy, Nancy, France (in French).